Numerical Modeling of Flashing Sprays Using a Hybrid Breakup Model

Yağmur Güleç[1], Alvaro Diez[1*] and Francesco Contino[2]

[1] *Mechanical Engineering Department, Izmir Institute of Technology, Izmir, Turkey*
[2]*Vrije Universiteit Brussel, Brussels, Belgium*

Abstract

Fuel droplets may undergo flash-boiling conditions when they are injected into a cylinder at higher than saturation temperature for the corresponding chamber pressure, resulting in a rapid evaporation. Such conditions lead to wider spray angles, finer droplets and shorter penetration. Based on current investigations, such conditions may promote a more homogeneous fuel-air mixture and a faster evaporation compared to traditional methods.

This investigation presents a numerical study in OpenFOAM focusing on the modeling of gasoline direct injection sprays under flash and non-flash boiling conditions. The model was implemented in a scenario where already superheated and compressed n-heptane fuel at 100 bar was injected into a chamber at a pressure lower than its saturation pressure at the corresponding temperature. This scenario has been additionally implemented to the code alongside the scenario in which the fuel goes through the flashing conditions by taking heat from the ambient.

A new hybrid breakup method has been implemented along with a momentum flux post-processing tool for the characterization of the initials conditions.

It was found that better prediction accuracy in evaporation rate was obtained. Spray penetration was also better modeled for flash boiling conditions compared with traditional breakup models.

Keywords: Breakup of droplets; Discharge coefficient; Flash boiling; Injection velocity; Momentum flux; Spray modeling.

* Corresponding author
Alvaro DIEZ
alvarodiez@iyte.edu.tr
Address: Mechanical Engineering Department, Izmir Institute of Technology, Gulbahce Campus, Izmir, Turkey
Tel:+902327506706
Fax: +903122028639

_____

1. Introduction

The use of direct injection, together with downsizing and boosting is considered a promising technique to reduce fuel consumption in spark-ignited engines. Researchers have been developing high pressure injectors to reveal the potential of this technology. Such injectors however generate faster sprays, increasing the risk of piston wall impingement and therefore resulting in unburned hydrocarbon emissions [1] .

The idea to generate fast vaporizing and low penetrating sprays has encouraged investigation of the conditions providing rapid evaporating sprays. In commercial gasoline direct injection engines, the temperature of injector body may reach up to 200°C. When these conditions are combined with early intake valve closure, the compressed fuel at injection undergoes a rapid phase change since the pressure surrounding the fuel significantly drops to sub-atmospheric values. As a result, flashing phenomenon occurs either when spray is heated to a temperature higher than the saturation temperature at that pressure or already superheated spray corresponding to the chamber pressure de-pressurized immediately. In this case, the main character is internal heat transfer from the droplet core to the surface, which causes the temperature to drop to the saturation temperature and become superheated as soon as the droplet emerges from the injector. Flash boiling conditions cause a thermodynamic breakup, which results in smaller droplets and faster evaporation. Under such conditions, the latent heat is used up by bubble nucleation [2]. Bubble nucleation can grow until the fuel goes into a stable state from a metastable state. Consequently, the catastrophic breakup of the liquid alters the spray morphology dramatically with the reduced droplet sizes and enhanced evaporization rates [3-5] under flashing conditions. With finer droplets formed [3], a reduction of unburned hydrocarbons and soot emissions may occur. Furthermore, a better fuel-air mixture thanks to

enhanced atomization allows increased combustion efficiency.

Open source CFD codes such as OpenFOAM have recently gained more interest by researchers from academy since the accessibility of the source codes enables the implementation of new models into already existing models and the development of advanced models [6–9].

In addition to the evaporation phenomena, the breakup mechanisms of a spray are one of the most important considerations for spray simulations. In the Lagrangian frame, there are various models for simulating the primary and secondary breakup of droplets. Both atomization and secondary breakup are considered depending on different spray regions based on the liquid fraction. For those studies whose injector geometries are unknown, the effect of in-nozzle flow, in terms of cavitation and turbulence, may be simulated for some phenomenological atomization models employed in user-defined denser spray region along with an independent secondary model. The Kelvin-Helmholtz Rayleigh-Taylor (KH-RT) breakup model that takes into account the instabilities due to acceleration and the Kelvin-Helmholtz instabilities caused by aerodynamic forces has been widely employed in diesel sprays.

When compared to high-pressure spray, flash-boiling sprays emerging from the nozzle at medium range injection pressure, break up in a shorter time. Thus, existing breakup models may not predict the measured penetration lengths for the low-to-medium injection pressure conditions accurately. Several numerical studies have been carried out for gasoline direct injection sprays [10–13], Thus in [10], the rate at which droplets fragmented was performed as a function of the Weber number, We.

Chryssakis and Assanis proposed and applied a hybrid approach [14], using the primary breakup model of Huh et al. [15], which had been employed and tested for both diesel and hollow cone Gasoline Direct Injection (GDI) sprays for varying conditions. Another hybrid breakup model (KH-ACT) by Som and Aggarwal [16] was developed based on the fact that cavitation, turbulence or aerodynamic forces may be the most dominant reasons for the primary breakup. They drew a comparison between the conventional KH model with the KH-ACT model, resulting in shorter liquid penetration. The new breakup model exhibited a better agreement with experimental penetration results for diesel sprays.

In other GDI sprays studies ([6], [11], [17]), the Rosin Rammler distribution has been widely used since the bulk liquid is assumed to have already been fragmented into smaller droplets obeying a probabilistic distribution.

In the study of Rotondi et al. [10] the combination of the Taylor Analogy Breakup (TAB) [18] model and the WAVE model was applied. They showed the existence of great number of droplets with the We number lower than 12. Thus the TAB model processed the breakup of droplets with the Weber number lower than 12. This resulted in bet-

ter prediction of the liquid penetration.

Cavicchi et al. [17] employed a reasonable Rosin-Rammler distribution matching with experimental penetration results for the primary breakup of the bulk liquid instead of the blob method. For the secondary breakup, they applied the Reitz-Diwakar breakup model [19] and then they validated their model against momentum flux measurements.

The current study aimed to prepare a CFD model for flashing sprays. The evaporation model takes into consideration of the experimental correlation between evaporation rate and superheat degree (difference droplet temperature and boiling temperature) proposed by Zuo et al. [12]. In the scenario where the sprays undergo flashing conditions by de-pressurization has been implemented. Furthermore, a momentum flux post-processing tool has been developed for the calculation of initial velocity in case discharge coefficient are not revealed experimentally and lastly the TAB and Pilch Erdman correlations were combined as a hybrid model. Consequently, better prediction accuracy in evaporation rate regarding the superheat degree, initial injection velocity and breakup phenomenon under flash and non-flash boiling conditions has been obtained.

2. Numerical Setup

In this study, a Lagrangian-Eulerian solver called sprayFoam, which is one of the compressible and PIMPLE solvers in OpenFOAM was used coupled with the standard k-ε turbulence equations. While parcels, representative for identical spray droplets, are being tracked, they exchange mass, momentum and energy with a computational cell.

Parcels with the experimentally determined spray angle are injected at the outlet of the injector. Initial droplet size distribution is assumed to obey the Rosin-Rammler distribution with spread parameter q=3 at the range between 1 μm and 200 μm, which has been widely used for modeling droplet size distribution of both diesel and gasoline sprays ([6], [10], [20]) . The spray has been assumed to fragment into droplets initially with certain size distribution. Initial diameter sizes were represented as a Rosin Rammler distribution at the range between 1e-6 and 1e-4 m, which has Sauter Mean Diameter (SMD) of 50 μm According to the photographic study by Reitz [21], the fact of reduction in droplet size in the vicinity of the injector and outer regions was observed.

2.1 Injection Rate and Injection Velocity

A trapezoidal mass flow rate injection profile at 100 bar injection pressure was implemented, as shown in Fig. 1.
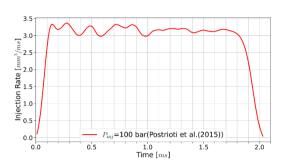
Fig. 1. Injection profile at 100 bar injection pressure.

The injection parameters employed in this study are shown in Table 1 [22]. The operating conditions such as fuel temperature and back pressure are reported in Table 2. The operating cases have comprised of both flash and non-flash boiling conditions.

Table 1. Injection parameters.

Fuel	n-heptane
Injection pressure (bar)	100
Total Injected Mass (mg)	3.5-4
Injection duration (ms)	2

The tendency of flash boiling conditions were indicated in [1] depending on the ratio of air pressure to saturation pressure (AtSPR). Thus, when the ratio is lower than 0.3, full flash boiling conditions appear, when the value varies between 0.3 and 1, it implies that the case is under partial flash boiling conditions, whereas if the AtSPR is higher than 1, it is interpreted as non-flash boiling.

Table 2. Injection parameters.

Cases	T_f (K)	P_v (bar)	AtSPR
1	300	0.4	8.47
2	363	0.4	0.51
3	393	0.4	0.22
4	393	1	0.55
5	393	3	1.65

As a flow rate is implemented into the model, the initial droplet velocity is calculated as follows:

$$U_{init} = \frac{\dot{m}(t)}{\rho_l C_d A_n}, \qquad (1)$$

where A_n stands for the nozzle hole area and C_d is the discharge coefficient for the contraction of the nozzle hole.

For the initial velocity estimation, the discharge coefficient values of 0.45 and 0.5 were used by means of compar-

ing the numerical momentum flux with the data measured at 10 mm from the injector as shown in Fig. 9 by [22]. The optimum value was selected according to the post-processing of momentum flux shown in Sec. 3.

2.2. Mesh

Grid size dependency was tested with three grid resolutions. The coarse mesh contained 60000 computational cells, the mesh configuration at medium level contained 180000 cells while the finest mesh configuration was generated with 400000 cells. Cell size was varied from 1 to 1.5 mm in the coarse mesh configuration (see Table 3) ensuring convergence. In addition, cell sizes were at the range of 0.6-0.7 mm in the higher mesh resolution. The liquid penetration was calculated for these cases, as shown in Fig. 2. As it can be seen, the medium and fine meshes gave similar results, while the coarse mesh configuration underestimated the penetration. Considering time costs, the medium grid resolution was applied to all simulations. This configuration contained cells ranging from 0.7 and 1 mm in size in a cylindrical domain, as depicted in Fig. 3. The simulations were done with a time-step of 1 μs as proposed by Zuo et al. [12] for fast evaporating cases.

Table 3. Computational mesh configuration.

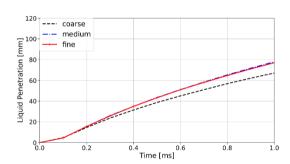|	Number of cells	Mesh sizes
coarse	60000	1-1.5 mm
medium	180000	0.7-1.3 mm
fine	400000	0.6-0.7 mm

Fig. 2. Grid dependency analysis for fully flash boiling condition (T_f=393 K and P_v=0.4 bar).

2.3 Submodels

In this work, sub-models have been enabled for evaporation, breakup and drag force calculation exerted on droplets in the spray. A new hybrid breakup in which the TAB and Pilch Erdman correlations have been combined was employed for spray penetration calculation for full flash boiling, partial and non-flash boiling conditions.
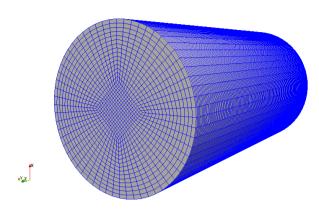
Fig. 3. Computational mesh (medium).

2.3.1 Superheated Evaporation Model

The evaporation model proposed by Zuo et al. [12] was applied to the model. It takes into account heat transfer from the superheated droplet itself apart from heat transfer from the surrounding environment. The internal heat flux Q_1 is based on the experimental correlations as the heat transfer coefficient α, where ΔT is the superheat degree defined as $T_d - T_b$ and H_v is the latent heat of the fluid.

$$Q_1 = \pi \alpha d_d^2 (T_d - T_b) \qquad (2)$$

At superheated conditions, the total evaporation rate M_t is the summation of subcooled M_{sc} and superheated evaporation rates M_{sh}.

$$\frac{dM_t}{dt} = \frac{dM_{sc}}{dt} + \frac{dM_{sh}}{dt}, \qquad (3)$$

where subcooled evaporation rates are calculated as follows:

$$\frac{dM_{sc}}{dt} = d_d \pi \rho D \ln(\frac{1-Y_{f,\infty}}{1-Y_{f,R}}) Sh, \qquad (4)$$

where Sh is the Sherwood number, it accounts for increased mass transport due to the relative velocity between the droplet and the gas surrounding the droplet. D is the diffusivity coefficient of the fuel vapor in air, $Y_{f,R}$ is the fuel vapor mass fraction at the droplet surface, while $Y_{f,\infty}$ accounts for fuel vapor mass fraction outside the boundary layer. In addition, the heat transfer coefficient α in Eq. 2 is proposed as a function of the superheat degree ΔT as follows:

$$\alpha = \begin{cases} 760\Delta T^{x_1}, & 0 < \Delta T < 5 \\ 27\Delta T^{x_2}, & 5 < \Delta T < 25 \\ 13800\Delta T^{x_3}, & \Delta T > 25 \end{cases}$$

where the heat transfer exponents were proposed as $x_1 = 0.26, x_2 = 2.33, x_3 = 0.39$ [12]. The superheated evaporation rate is calculated as follows based on Eq. 2:

$$\frac{dM_{sh}}{dt} = \frac{Q_1}{H_v}, \qquad (5)$$

2.3.2 Hybrid Breakup Model

The droplet breakup is driven mainly by the disruptive aerodynamic forces and the restorative surface tension forces. The ratio of aerodynamic forces to the surface forces is represented by the Weber number in Eq. 6.

$$We = \frac{\rho_g U_r^2 d}{\sigma_l} \qquad (6)$$

The larger the We number, the larger the droplets tendency towards breakup. The We number has a key role for the determination of breakup modes as proposed by Pilch and Erdman [23]. The correlations categorized five different breakup regimes depending on the We, as shown in Eq. 7.

$$\begin{aligned} T_{bu} &= 6(We-12)^{-0.25} & 12 < We < 18 \\ T_{bu} &= 2.45(We-12)^{0.25} & 18 < We < 45 \\ T_{bu} &= 14.11(We-12)^{-0.25} & 45 < We < 351 \\ T_{bu} &= 0.766(We-12)^{-0.25} & 351 < We < 2670 \\ T_{bu} &= 5.5 & We > 2670 \end{aligned} \qquad (7)$$

where T_{bu} is is the non-dimensional breakup time. The characteristic breakup time τ_{bu} is given by:

$$\tau_{bu} = T_{bu}(\frac{\rho_l}{\rho_g})^{0.5}(V_r / d) \qquad (8)$$

In addition to the We number, the Ohnesorge number is a representative of the ratio of drop viscous forces to surface tension forces. Drop viscosity results in less energy dissipation by aerodynamic forces. Consequently, droplets are highly unlikely to be deformed under high viscous forces.

$$Oh = \frac{\mu_l}{\sqrt{\rho_l d_0 \sigma}} \qquad (9)$$

In the present study, the TAB and Pilch Erdman correlations were combined as a hybrid model as reported in Table 4.

4

Table 4. Hybrid breakup model as a function of the We number, [10].

TAB Model	$We < 12$
Vibrational mode	$12 < We < 18$
Bag regime	$18 < We < 45$
Chaotic regime	$45 < We < 100$
Stripping regime	$100 < We < 1000$
Catastrophic regime	$We > 1000$

2.3.3 Dynamic Drag Model

The equation of motion for a droplet is written depending on the drag force acting on the droplet as follows:

$$\frac{d^2 X}{dt^2} \rho_l V = C_D A_f \rho_g U_r^2 / 2 \qquad (10)$$

where V, A_f and X are the volume, frontal area and position of a drop, respectively. U_r stands for relative velocity between the gas and liquid phase. The drop drag coefficient is given for a rigid sphere as in Eq. 11 below:

$$C_{D,sphere} = \begin{cases} \dfrac{24}{Re}(1 + 1/Re^{2/3}) & Re < 1000 \\ 0.424 & Re > 1000 \end{cases} \qquad (11)$$

where the Reynolds number is defined as follows:

$$Re = \frac{\rho_g U_r d}{\mu_g} \qquad (12)$$

However, when a drop moves into ambient conditions, it will have no longer a spherical shape due to distortion and deformations. These deformations were combined with the TAB model [15], predicting the deformation from sphere to disk. Thus, a new drag coefficient was defined as:

$$C_D = C_{D,sphere}(1 + 2.632y) \qquad (13)$$

where $C_{D,sphere}$ is given in Eq 11. Drop distortion y is calculated by the TAB model by [18] which was activated in the model's algorithm.

3. Preliminary Results and Contribution to the Model

Different scenarios may lead for injected fuel to go through flashing conditions. In the first scenario, the fuel is injected at relatively low temperatures into an ambient at a higher temperature (the point 3 in Fig. 4) and then it absorbs heat from the surrounding (the point 4 in Fig. 4). The second scenario includes the already superheated fuel, injected into the combustion chamber at lower pressure than the saturation pressure at the concerning temperature (from point 1 as a compressed liquid at 100 bar in Fig. 4 to point 2). In OpenFOAM, the temperature is limited to boiling temperature shortly after the fuel has been injected, as the parcel definition was designed in a way that the first scenario was considered. As a result, there is no superheat degree and droplets are not treated as if they are boiling. In disabling the limitation of temperature to the boiling temperature, designed for fuels undergoing after taking heat from their surroundings, superheat degree was taken into consideration. Thus the temperature-time profile where examined in Fig. 5. It shows the comparison of the standard model with the modified model for two parcels with initially same mass under full flash boiling conditions ($T_f = 393$ K and $P_v = 0.4$ bar). As it can be seen the droplet temperature decay follows a more normal curve when compared to the standard model, in which temperature is immediately dropped to the boiling temperature.

The enhanced temperature profile has led the droplet to be treated as boiling fuel and to be taken at superheat degree, which enabled the evaporated mass to be computed by Eq. 5. The evaporation rate for a parcel with initially injected with the same mass and diameter was significantly higher in the modified model, as expected. While the droplets processed by the new model used up virtually all their mass, the droplets treated conventionally had still liquid mass inside itself, as shown in Fig. 6.
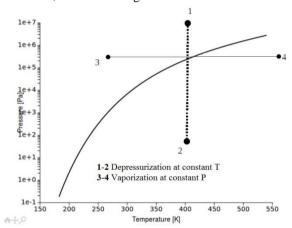
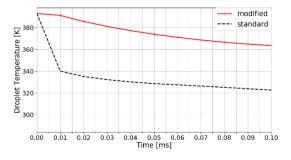

Fig. 4. N-heptane p-v diagram [24].

Fig. 5. Droplet temperature- time profile.

The enhanced evaporated mass-time profile for two par-

cels with initially the same mass and vapor mass fraction in the cross section was compared for the standard model and the new evaporative model at 0.7 and 0.9 ms after the start of injection (aSOI). The effect on the area of fuel in gas phase is shown in Figs. 7 and 8. They show the vapor footprint area and the mass fraction of vapor on the spray axis respectively, comparing the standard and modified model. The new model resulted in slightly higher evaporation rate compared to the standard model results.
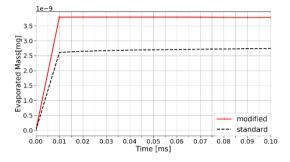

Fig. 6. Evaporated mass-time profile .

Two further modifications have been implemented in the OpenFOAM model: the first related to the hybrid breakup model (see Sec. 2.3.2 for further details) and the post-processing of momentum flux calculation across a plane. For the initial velocity calculation discharge coefficient is a very important parameter. In this study the value of the C_d was not available, so a preliminary study was carried out to find out the optimal value. This was done by looking at the fuel momentum flux data that was available in [22].
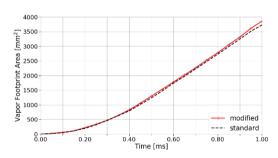

Fig. 7. Vapor footprint area.

They applied a computational model for diesel injection as free-jet (virtual target) and target configurations. They proposed the formulation (see Eq. 14) under transient conditions, similar to real engine-like conditions, for free-jet case to compare the impact force measured at a certain distance from the injector. The proposed formulation was found useful to be applied under unsteady conditions since steady conditions may be only reached after 2 ms aSOI.
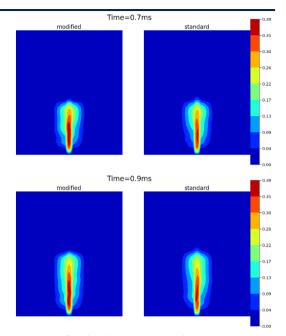

Fig. 8. Vapor mass fraction in the cross section 0.7 and 0.9 ms aSOI.

$$F = \int p \, ds + \iint \rho v_z^2 \, ds + \dot{M}_{z,droplet}, \qquad (14)$$

where the integrals are over the area of the plane at distance 10 mm from injector. Subscript z stands for the injection direction. The momentum flow rate of liquid phase through a virtual plane can be computed applying Eq. 15.

$$F_d(t) = \sum_{i=1}^{N_d} m_d(t)V_z(t) / \tau, \qquad (15)$$

N_d accounts for number of droplet impacting on the plane, τ is proposed as the time range between 5e-6 and 2e-5 s.

Thus a comparison was made between the experimental momentum flux measured at 10 mm from the injector as shown in Fig. 9 for the case at 300 K fuel temperature and 0.4 bar chamber pressure. The discharge coefficient values of 0.45 and 0.5 were employed in this comparison and it was found the optimum value of 0.45, where both momentum flux and liquid penetration were in better agreement, as shown in Fig. 10. Consequently a C_d of 0.45 was used for the rest of this study.
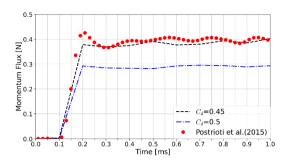
Fig. 9. Momentum flux at 10 mm distance from the tip of the injector.
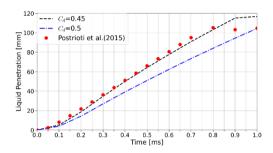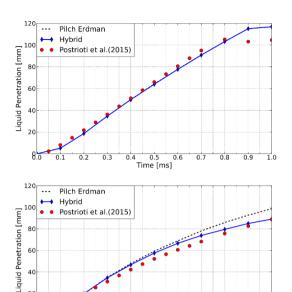

Fig. 10. Effect of C_d on liquid penetration.

4. Results

The newly implemented model, with the hybrid breakup model was then tested against the experimental data and the Pilch Erdman correlations for both flash boiling and non-flash boiling conditions. Fig. 11 depicts the liquid spray penetration for the three approaches for the same chamber pressure of $P_v = 0.4$ bar with three fuel temperatures $T_f = 300$ K (top), $T_f = 363$ K (center) and $T_f = 393$ (bottom), representing non-flash boiling, transition and full flash boiling conditions respectively. In addition, the same initial droplet size was used for flash and non-flash boiling cases. The hybrid breakup model showed good agreement with the experimental data for the flashing cases when the spray was fully developed. There was a slight penetration underestimation between 0.2 and 0.7 ms aSOI Fig. 11 (bottom). For the transition case, where some flashing phenomena have been observed experimentally, the liquid penetration was, in fact, very well predicted. For the non-flashing case (top), both the hybrid model and the Pilch Erdman correlations were able to predict the penetration accurately. Just after 1 ms of injection the models and experimental data differ, this could because the model still accounts for the small liquid droplets to keep traveling while in the experimental data, the fine droplets at the tip of the injector may not be observed under that Mie scattering setup.
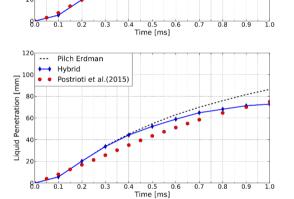

Fig. 11. Liquid penetration at $P_v = 0.4$ bar and $T_f = 300$ K (top), $T_f = 363$ K (center) and $T_f = 393$ K (center).

The reason why the hybrid breakup models have given closer numerical results for flash boiling cases, lies in the fact that the interaction between air and liquid is higher with the hybrid breakup model. As seen in Fig. 12, the air momentum flux is higher for the hybrid model. Only, at the closest location to the injector of 20 mm the two models show similar results. For the rest, the more drag force exerted on droplets cause them to slow down, which resulted in better predictions with the hybrid breakup model (dash line with symbols in Fig. 12 for the fully flashing case. In Fig. 12 the lines without symbols accounts for the results run with the Pilch Erdman breakup model.
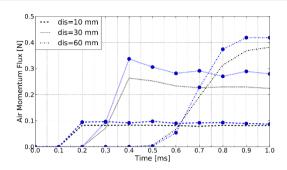
7

Fig. 12. Air momentum flux for in the injection direction across planes at 10, 30 and 60 from the injector with Pilch Erdman breakup model (dash lines) and hybrid breakup model (dash line with symbols) ($P_v = 0.4$ bar and $T_f = 393$ K).

The numbers of particles during the breakup appears to increase in the hybrid breakup model. It increased significantly four times the number processed by the Pilch Erdman breakup model 0.1 ms aSOI. However, this significant increase in the number of particles could not be seen for the cases at lower fuel temperature. Consequently, the penetration results did not make a substantial difference as shown in Fig. 11(top).

Fig. 13 depicts the liquid spray penetration for the same fuel temperature $T_f = 393$ K for two more chamber pressure of $P_v = 1$ bar (top) and $P_v = 3$ bar (bottom). These two cases represent partial flash boiling and non-flash boiling condition respectively. For the partial flash boiling conditions both hybrid and Pilch Erdman models give similar results, with the hybrid model showing a slight under prediction after 0.7 ms aSOI. For the non-flash boiling case, the penetration results differ in higher magnitude. This was because the hybrid model presented droplet with higher drag coefficents as the ambient pressure was increase, slowing down the spray penetration.
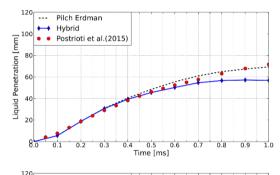
5. Conclusion and Future Work

The current numerical framework was aimed to predict the global spray shape under flash boiling conditions. At first, an evaporation model, which takes into account the superheat degree was made functional for flashing fuels injected at high temperature into a chamber at lower temperature. A momentum flux calculation was employed for the determination of the initial conditions. Furthermore, a hybrid breakup model was applied, which reduced the average droplet diameter due to higher level of breakup. As a result, the liquid penetration under for flashing conditions was better predicted when compared to traditional models.

The numerical model with enabled droplet distortion calculations was matched with measured liquid data for flashing sprays at 0.4 and 1 bar chamber pressures whereas for higher vessel pressure of 3 bar, it resulted in over estimation of liquid penetration. This over estimation can be attributable to the direct effect of the air density, which may result in

nonphysical drag force exerted on droplets. Moreover, the study has not investigated the initial droplet distribution depending on the conditions. Instead, the same initial droplet distribution has been employed for all cases. Therefore, there may be lacking physical consideration from this point of view.

As a future work, the consideration in which droplet distribution depending on both different chamber pressures and superheat degree for flashing cases is a good focus. In addition to this, Eulerian and Lagrangian solvers can be coupled with each other so that one can switch another depending on spray regions, which may give better results for the non-flash boiling cases particularly. Considering the real engine conditions with piston movements, spray-wall interactions should also be included alongside other sub-models used in the present study.
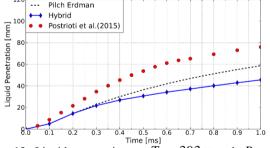

Fig. 13. Liquid penetration at $T_f = 393$ K and $P_v = 1$ bar (top) and $P_v = 3$ bar (bottom).

Acknowledgement

Nomenclature

C_d	: discharge coefficient
C_D	: drag coefficient
T_f	: fuel temperature
P_v	: chamber pressure
P_{inj}	: injection pressure
Re	: Reynolds number
We	: Weber number

U_r	: relative velocity between droplet and air
d	: droplet diameter
ρ_g	: gas density
ρ_l	: liquid density
μ_l	: liquid dynamic viscosity
σ_l	: surface tension

References

[1] Xu, M., Zhang, Y., Zeng, W., Zhang, G., and Zhang, M. (2013). Flash boiling: easy and better way to generate ideal sprays than the high injection pressure. *SAE International Journal of Fuels and Lubricants,* 6(1), 137-148.

[2] Ashgriz, N. (Ed.). (2011). Handbook of atomization and sprays: theory and applications. S*pringer Science & Business Media.*

[3] Kale, R., and Banerjee, R. (2017). Influence of Engine like Conditions on Macroscopic as well as Microscopic Spray Behavior of GDI Injector Using Isooctane and Alcohols. *SAE Technical Paper* (No. 2017-01-0855).

[4] Allocca, L., Montanaro, A., Di Gioia, R., and Bonandrini, G. (2014).Spray characterization of a single-hole gasoline injector under flash boiling conditions . *SAE Technical Paper* (No. 2014-32-0041).

[5] Guo, H., Li, Y., Shen, Y., and Zhang, Z. (2018). Characterizing Propane Flash Boiling Spray from Multi-Hole GDI Injector. *SAE Technical Paper,* 01-0278.

[6] Huang, C., and Lipatnikov, A. (2011). Modelling of gasoline and ethanol hollow-cone sprays using OpenFOAM . *SAE Technical Paper* (No. 2011-01-1896).

[7] Kim, D., & Kim, K. (2014). Comparison of Spray Structures of Diesel and Gasoline Using Modified Evaporation Model in Openfoam CFD Package. *SAE Technical Paper* (No. 2014-01-1417)

[8] Yu, S., Yin, B., Jia, H., and Yu, J. (2017). Numerical research on micro diesel spray characteristics under ultra-high injection pressure by Large Eddy Simulation (LES). Inter*national Journal of Heat and Fluid Flow,* 64, 129-136.

[9] Kösters, A., and Karlsson, A. (2011). A comprehensive numerical study of diesel fuel spray formation with openfoam . *SAE Technical Paper* (No. 2011-01-0842).

[10] Rotondi, R., Hélie, J., Leger, C., Mojtabi, M., and Wigley, G. (2010, September). Multihole gasoline direct injection spray plumes. In 23rd Annual Conference on Liquid Atomization and Spray Systems, Brno, Czech Republic.

[11] Li, Z. H., He, B. Q., & Zhao, H. (2014). Application of a hybrid breakup model for the spray simulation of a multi-hole injector used for a DISI gasoline engine. *Applied Thermal Engineering,* 65(1-2), 282-292.

[12] Zuo, B., Gomes, A. M., & Rutland, C. J. (2000). Modelling superheated fuel sprays and vaporization. *International Journal of Engine Research,* 1(4), 321-336.

[13] Price, C., Hamzehloo, A., Aleiferis, P., & Richardson, D. (2015). Aspects of numerical modelling of flash-boiling fuel sprays . *SAE Technical Paper* (No. 2015-24-2463).

[14] Chryssakis, C., and Assanis, D. N. (2008). A unified fuel spray breakup model for internal combustion engine applications. *Atomization and Sprays,* 18(5).

[15] Huh, K. Y., Lee, E., and Koo, J. (1998). Diesel spray atomization model considering nozzle exit turbulence conditions. *Atomization and Sprays,* 8(4).

[16] Som, S., & Aggarwal, S. K. (2010). Effects of primary breakup modeling on spray and combustion characteristics of compression ignition engines. *Combustion and Flame,* 157(6), 1179-1193.

[17] Cavicchi, A., Postrioti, L., Giovannoni, N., Fontanesi, S., Bonandrini, G., and Di Gioia, R. (2017). Numerical and experimental analysis of the spray momentum flux measuring on a GDI injector. *Fuel*, 206, 614-627.

[18] O'Rourke, P. J., & Amsden, A. A. (1987). The TAB method for numerical calculation of spray droplet breakup . *SAE Technical Paper* (No. 872089).

[19] Reitz, R. D., & Diwakar, R. (1986). Effect of drop breakup on fuel sprays . *SAE Technical Paper* (No. 860469).

[20] M. C. V., Buscaglia, G., Dari, E., & Zamonsky, O. Modeling Mixture Formation In A GDI Engine.

[21] Reitz, R. D. (1990). A photographic study of flash-boiling atomization. *Aerosol Science and Technology,* 12(3), 561-569.

[22] Postrioti, L., Bosi, M., Cavicchi, A., Abuzahra, F., Di Gioia, R., and Bonandrini, G. (2015). Momentum flux measurement on single-hole GDI injector under flash-boiling condition. *SAE Technical Paper* (No. 2015-24-2480).

[23] Pilch, M., and Erdman, C. A. (1987). Use of breakup time data and velocity history data to predict the maximum size of stable fragments for acceleration-induced breakup of a liquid drop. *International journal of multiphase flow*, 13(6), 741-757.

[24] Bell, I. H., Wronski, J., Quoilin, S., and Lemort, V. (2014). Pure and pseudo-pure fluid thermophysical property evaluation and the open-source thermophysical property library CoolProp. *Industrial & engineering chemistry research,* 53(6), 2498-2508.